

See discussions, stats, and author profiles for this publication at: <https://www.researchgate.net/publication/256478526>

# Aqueous Mg<sup>2+</sup> and Ca<sup>2+</sup> Ligand Exchange Mechanisms Identified with 2DIR Spectroscopy

ARTICLE *in* THE JOURNAL OF PHYSICAL CHEMISTRY B · SEPTEMBER 2013

Impact Factor: 3.3 · DOI: 10.1021/jp407960x · Source: PubMed

---

CITATION

1

READS

60

## 5 AUTHORS, INCLUDING:



[Wenkai Zhang](#)

University of Pennsylvania

22 PUBLICATIONS 328 CITATIONS

[SEE PROFILE](#)



[Robert W Hartsock](#)

Stanford University

16 PUBLICATIONS 166 CITATIONS

[SEE PROFILE](#)



[Kelly J Gaffney](#)

Stanford University

91 PUBLICATIONS 2,313 CITATIONS

[SEE PROFILE](#)

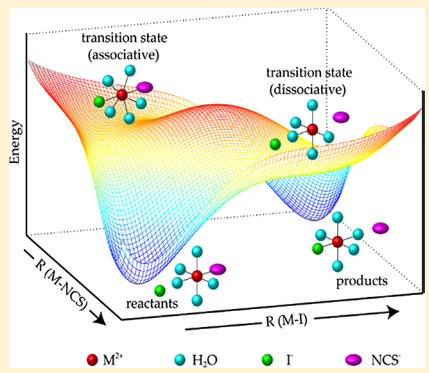
# Aqueous $Mg^{2+}$ and $Ca^{2+}$ Ligand Exchange Mechanisms Identified with 2DIR Spectroscopy

Zheng Sun, Wenkai Zhang, Minbiao Ji,<sup>†</sup> Robert Hartsock, and Kelly J. Gaffney\*

PULSE Institute, SLAC National Accelerator Laboratory, Stanford University, Stanford, California 94305, United States

## S Supporting Information

**ABSTRACT:** Biological systems must discriminate between calcium and magnesium for these ions to perform their distinct biological functions, but the mechanism for distinguishing aqueous ions has yet to be determined. Ionic recognition depends upon the rate and mechanism by which ligands enter and leave the first solvation shell surrounding these cations. We present a time-resolved vibrational spectroscopy study of these ligand exchange dynamics in aqueous solution. The sensitivity of the CN-stretch frequency of  $NCS^-$  to ion pair formation has been utilized to investigate the mechanism and dynamics of ligand exchange into and out of the first solvation shell of aqueous magnesium and calcium ions with multidimensional vibrational (2DIR) spectroscopy. We have determined that anion exchange follows a dissociative mechanism for  $Mg^{2+}$  and an associative mechanism for  $Ca^{2+}$ .



## I. INTRODUCTION

Calcium and magnesium cations have many chemical similarities in aqueous solution, yet significantly different roles in biochemical processes. Biological systems also regulate these cations by excluding  $Ca^{2+}$  from the cytosol, while allowing  $Mg^{2+}$  cations to enter. To achieve these distinct roles in biochemical processes and preferentially exclude  $Ca^{2+}$  from the interior of the cell, biological systems must distinguish  $Ca^{2+}$  and  $Mg^{2+}$  with high fidelity, but the mechanism for the distinction has yet to be conclusively determined. The central step of ion recognition should involve the interchange of ligands into and out of the first solvation shell of  $Mg^{2+}$  or  $Ca^{2+}$  cations.<sup>1</sup> This ligand exchange represents the central reaction in inorganic synthesis and a critical reaction in catalysis. In analogy with the  $S_N1$  and  $S_N2$  reaction mechanisms of organic chemistry, ligand exchange reactions can be characterized as associative or dissociative, where an  $S_N1$ -like dissociative ligand exchange reaction involves a hypocoordinated metal center transition state and an  $S_N2$ -like associative reaction involves a hypercoordinated metal center transition state.<sup>2,3</sup>

Extensive experimental<sup>2–6</sup> and simulation<sup>7–11</sup> studies of water molecule exchange into and out of the first solvation shell of alkali and alkali earth cations in aqueous solutions highlight the difficulty in acquiring an atomic scale understanding of chemical reactivity. While simulation studies provide the most detailed information, changes in the simulation methodology and data analysis procedures lead to significant variation in the equilibrium between the free ions and the contact ion pairs<sup>10</sup> and in water residence times,<sup>7–9</sup> and have arrived at exchange mechanisms distinct from those inferred from experiment, at least for the case of aqueous  $Ca^{2+}$  cations.<sup>4,12</sup>

We present a time-resolved IR spectroscopy investigation of ligand exchange dynamics in concentrated mixed ionic

solutions.<sup>13–25</sup> The high concentration ensures the close proximity of reactants, effectively eliminating diffusion from the observed reaction dynamics. The CN-stretch absorption of thiocyanate ( $NCS^-$ ) provides a clear sensor of the local coordination environment in aqueous solution. Under certain circumstances, the CN-stretch frequency provides a probe of the local electrostatic environment.<sup>26–29</sup> Stronger intermolecular interactions, such as contact ion pair formation or hydrogen bond formation to the nitrile group, lead to shifts in the CN-stretch frequency that cannot be accounted for with the Stark effect.<sup>26,27,30,31</sup> For the specific case of CIP formation between  $Mg^{2+}$  or  $Ca^{2+}$  and  $NCS^-$ , the blue shift results, at least in part, from perturbation of the resonance structures and bonding in the thiocyanate anion.

These distinct vibrational transition energies for the contact ion pairs (CIP) and the free anion configurations provide the opportunity to use 2DIR spectroscopy to investigate the equilibrium dynamics of ion association and dissociation in aqueous ionic solutions.<sup>15,19,20,32,33</sup> We present a multidimensional vibrational (2DIR) spectroscopy<sup>34–37</sup> study of the dynamics of anion exchange in aqueous magnesium and calcium solutions. Being a time domain measurement primarily sensitive to nearest neighbor interactions, 2DIR spectroscopy provides a new perspective to the study of ion–ion interaction in aqueous solution<sup>15,38</sup> that complements prior studies and has the potential to provide incisive tests of molecular dynamics studies.<sup>16–18,25</sup>

Our 2DIR measurements show clear evidence for exchange between the free thiocyanate and the CIP configurations, but

Received: August 8, 2013

Revised: September 5, 2013

Published: September 9, 2013



ACS Publications

© 2013 American Chemical Society

12268

dx.doi.org/10.1021/jp407960x | J. Phys. Chem. B 2013, 117, 12268–12275

these dynamics can originate from five different processes: transient heating,<sup>15</sup> energy exchange,<sup>23</sup> and three distinct chemical exchange reactions. Park et al. demonstrated previously that thermally induced signals contribute to the 2DIR spectra for time delays in excess of 50 ps<sup>15</sup> for concentrated aqueous ionic solutions, so we have eliminated transient solvent heating by limiting our study to time delays of  $\leq 40$  ps. This leaves four potential sources of the exchange dynamics observed in the 2DIR spectra: (A) energy transfer from a vibrationally excited NCS<sup>-</sup> in one configuration to a vibrational ground state molecule in the other configuration,<sup>23,39,40</sup> (B) the “self”-exchange of a vibrationally excited NCS<sup>-</sup> in either the free or the CIP conformation with a ground state NCS<sup>-</sup> in the opposite conformation, (C) anion exchange in the CIP between thiocyanate and the secondary anion in solution, and (D) anion–water exchange where the thiocyanate anion replaces a water molecule in the first solvation shell of a Mg<sup>2+</sup> or a Ca<sup>2+</sup> cation. While processes (A) and (B) cannot be easily distinguished, they can be easily eliminated by changing the thiocyanate concentration. A prior study by Sun et al.<sup>38</sup> showed that energy transfer and “self”-exchange do not influence the observed exchange dynamics for concentrations  $[NCS^-] \leq 0.4$  M. Distinguishing (C) anion exchange from (D) anion–water exchange proves more challenging. We have relied on a prior study of MgCl<sub>2</sub> and CaCl<sub>2</sub> solutions that show no evidence for MgCl<sup>+</sup> or CaCl<sup>+</sup> CIP formation for the cation concentration ranges we have investigated.<sup>41</sup> These solutions eliminate anion exchange as a possible mechanism for chemical exchange and also exhibit no chemical exchange on the tens of picoseconds time scale. For these reasons, we conclude that (C) anion exchange between thiocyanate and a secondary anion A<sup>-</sup> into and out of the first solvation shell of the alkali earth cation dominates the 2DIR measurements:



where M<sup>2+</sup> = Mg<sup>2+</sup> or Ca<sup>2+</sup>. In this prior study we used the sensitivity of the 2DIR spectra to anion exchange as an indirect monitor of MA<sup>+</sup> CIP formation, for a variety of secondary anions A<sup>-</sup> = Cl<sup>-</sup>, Br<sup>-</sup>, I<sup>-</sup>, NO<sub>3</sub><sup>-</sup> and ClO<sub>4</sub><sup>-</sup>. The present manuscript extends these prior studies by investigating the mechanism for anion entrance and exit from the first solvation shell of Mg<sup>2+</sup> and Ca<sup>2+</sup> and sets boundaries on the rate of water entrance and exit from the first solvation shell of Ca<sup>2+</sup>.

## II. EXPERIMENTAL METHODOLOGY

We built the 2DIR spectrometer using a design that has been described in detail elsewhere.<sup>42</sup> We use a Ti:sapphire oscillator (KM Laboratories) to seed a 1 kHz regenerative amplifier (Spitfire, Spectra-Physics). The amplifier generates 45 fs duration pulses with a central wavelength of 800 nm. We use  $\sim 1$  mJ per pulse to pump the first of two stages of optical parametric amplification to generate mid-IR pulses at 2050 cm<sup>-1</sup> by difference frequency generation. We measured the pulse chirp with frequency-resolved optical gating measurements in a transient grating geometry.<sup>42</sup> We used CaF<sub>2</sub> plates with different thicknesses to compensate for the linear dispersion introduced by other dielectric materials in the setup, particularly a Ge Brewster plate. This setup produced transform-limited mid-IR pulses with a  $\sim 250$  cm<sup>-1</sup> bandwidth (full width at half-maximum) and pulse durations of  $\sim 65$  fs at the sample. We utilize roughly 1  $\mu$ J pulse energies and focus the laser beams to roughly 50  $\mu$ m diameters in the sample.

The experimental details and principles of multidimensional vibrational correlation spectroscopy, generally termed two-dimensional infrared (2DIR) spectroscopy, have been described in detail elsewhere.<sup>37,42</sup> We purchased the salts and deuterium oxide from Sigma-Aldrich and used them as received. The experiments used a sample cell with two CaF<sub>2</sub> windows (3 mm thick) and a 6  $\mu$ m thick Teflon spacer to reduce the D<sub>2</sub>O background absorption.

## III. RESULTS

**A. FTIR Spectroscopy.** The linear triatomic thiocyanate anion (NCS<sup>-</sup>) has three IR-active vibrations, including the CN-stretching mode, which we probe in our 2DIR spectroscopy measurements.<sup>15,43,44</sup> Figure 1A shows the FTIR spectra in the

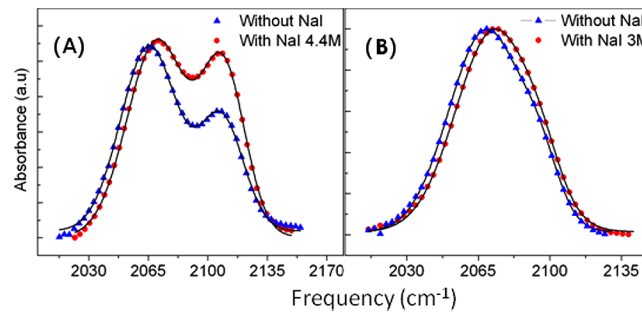


**Figure 1.** FTIR spectra in the spectral range of the CN-stretch of thiocyanate (NCS<sup>-</sup>) with the symbols showing the experimental data and the solid lines the fit of the experimental spectra to the sum of two Gaussian peaks. (A) FTIR spectra for 0.24 M NaNCS and 3.0 M MgI<sub>2</sub> solutions with 4.4 M NaI or no NaI. (B) FTIR spectra for 0.35 M NaNCS and 3.0 M CaI<sub>2</sub> solutions with 3 M NaI or no NaI. The absorption peak at 2115 cm<sup>-1</sup> in (A) corresponds to the CN-stretch absorption of NCS<sup>-</sup> in the MgNCS<sup>+</sup> CIP, while the shoulder at 2093 cm<sup>-1</sup> in (B) corresponds to the CaNCS<sup>+</sup> CIP. The absorption peak at around 2068 cm<sup>-1</sup> for all solutions corresponds to the CN-stretch absorption of water solvated NCS<sup>-</sup>.

CN-stretch region for two 0.24 M NaNCS, 3 M MgI<sub>2</sub> deuterated water solutions, one containing no NaI and the other containing 4.4 M NaI. Figure 1B shows the FTIR spectra for two 0.35 M NaNCS and 3.0 M CaI<sub>2</sub> deuterated water solutions, one containing no NaI and the other containing 3 M NaI. For low ionic concentrations, no CIP form in aqueous solution and only one CN-stretching absorption peak appears in the FTIR spectrum at 2068 cm<sup>-1</sup>. The situation changes for high concentrations of the larger charge density alkali earth cations, Mg<sup>2+</sup> and Ca<sup>2+</sup>. Aqueous solutions containing NCS<sup>-</sup> and Mg<sup>2+</sup> form N-bound 1:1 contact ion pairs, as well as water solvated anions. This leads to an additional CN-stretch absorption peak at 2115 cm<sup>-1</sup> for MgNCS<sup>+</sup> CIP, as shown in Figure 1A. The N-bound 1:1 contact ion pairs between Ca<sup>2+</sup> and NCS<sup>-</sup> have a CN-stretch absorption shoulder at 2093 cm<sup>-1</sup>, as shown in Figure 1B. The water solvated NCS<sup>-</sup> anions with a CN-stretch absorption peak at 2068 cm<sup>-1</sup> will be referred to as free NCS<sup>-</sup> anions, though the solvent separated ion pairs that exist in solution will also have a CN-stretch absorption peak that cannot be distinguished from free NCS<sup>-</sup> anions. Prior dielectric relaxation spectroscopy studies by Buchner et al. on aqueous Na<sub>2</sub>SO<sub>4</sub> solutions show that solvent separated ion pairs do not represent an appreciable fraction of the ions for concentrated ionic solutions.<sup>5,45</sup> This result

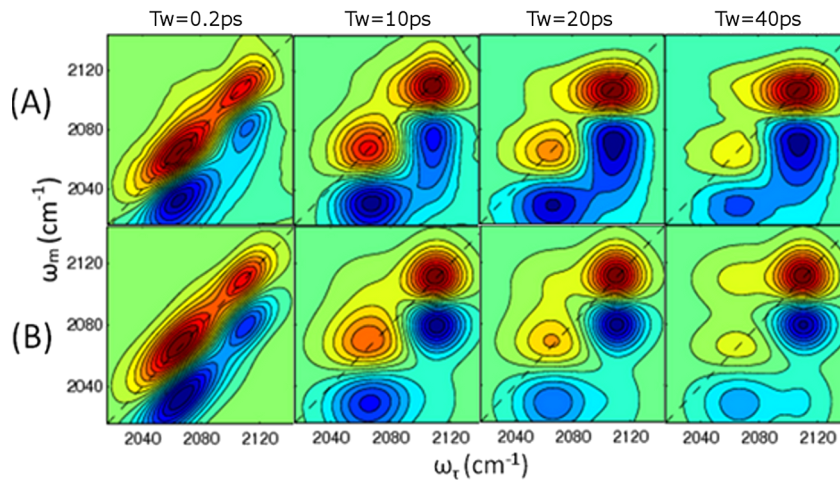


**Figure 2.** (A) Experimental and (B) simulated fit of the  $T_W$ -dependent 2DIR spectra of the CN-stretch of thiocyanate for aqueous solutions of 0.24 M NaNCS and 3 M MgI<sub>2</sub>. See text for description of the 2DIR spectra and Supporting Information for a description of the fitting procedure.

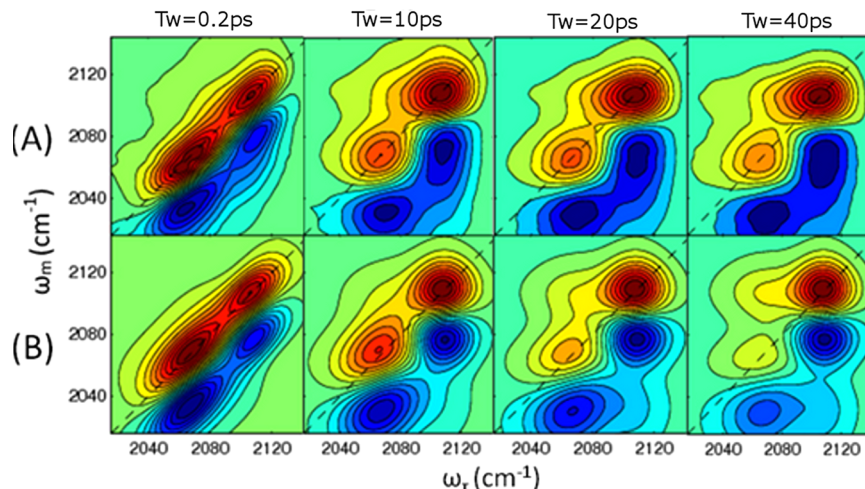


**Figure 3.** (A) Experimental and (B) simulated fit of the  $T_W$ -dependent 2DIR spectra of the CN-stretch of thiocyanate for aqueous solutions of 0.24 M NaNCS, 3 M MgI<sub>2</sub>, and 4.4 M NaI. See text for description of the 2DIR spectra and Supporting Information for a description of the fitting procedure.

indicates that anions and cations that do not form CIP move independently of one another in concentrated ionic solutions.

The relative intensity of the two CN-stretch absorption peaks in the FTIR spectrum reflects the equilibrium constant between the CIP and free configurations,

$$K = \frac{[\text{MNCs}^+]}{[\text{M}^{2+}][\text{NCS}^-]} \quad (2)$$

where  $\text{M}^{2+} = \text{Mg}^{2+}$  or  $\text{Ca}^{2+}$ . Quantitative determination of the concentrations of NCS<sup>-</sup> in the free and CIP configurations must account for the impact of CIP formation on the absorption cross-section. This can be determined from thiocyanate concentration dependent FTIR measurements or the relative intensities of the peaks in the FTIR and the diagonal peaks in the 2DIR spectrum for short waiting times. We have utilized this secondary method, which we discuss further in the Supporting Information.

**B. 2DIR Spectroscopy.** Ultrafast 2DIR spectroscopy monitors equilibrium ligand exchange dynamics on the picosecond time scale by labeling molecules through resonant excitation of the CN-stretch of NCS<sup>-</sup>, and then correlating

these initial frequencies,  $\omega_\tau$ , with the final stretch frequencies,  $\omega_m$ , associated with these same excited molecules after an experimentally controlled waiting time,  $T_W$ , analogous to the time delay in a pump-probe measurement. Figure 2A shows the absorptive 2DIR spectra for the 0.24 M NaNCS, 3 M MgI<sub>2</sub> solution, and Figure 3A shows the absorptive spectra for the a 0.24 M NaNCS, 3 M MgI<sub>2</sub>, and 4.4 M NaI solution.

The simulated fits to the experimental data appear in Figures 2B and 3B. The positive peaks shown in red along the diagonal ( $\omega_\tau = \omega_m$ ) result from vibrationally excited anions that do not change ion configuration during the  $T_W$  waiting time and emit an echo signal at the fundamental vibrational frequency,  $\nu = 0 \rightarrow 1$ . The high-frequency diagonal peak at  $\omega_\tau = \omega_m = 2115 \text{ cm}^{-1}$  results from vibrationally excited NCS<sup>-</sup> ions in the MgNCS<sup>+</sup> contact ion pair configuration, while the low-frequency diagonal peak at  $\omega_\tau = \omega_m = 2068 \text{ cm}^{-1}$  comes from the free NCS<sup>-</sup> ions. The negative peaks shown in blue below the diagonal arise from anions that do not change ion configuration during the  $T_W$  waiting time and emit an echo signal at the anharmonically shifted  $\nu = 1 \rightarrow 2$  transition. The 2DIR spectra also show cross peaks that correspond to vibrationally excited anions that undergo a change in ionic

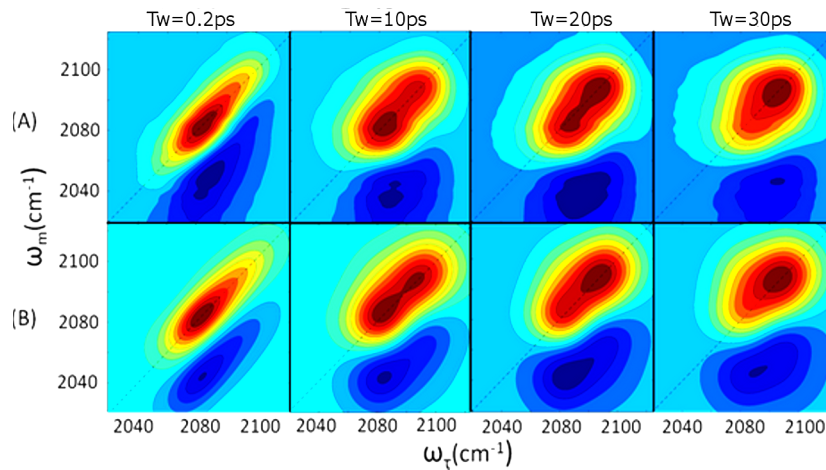


**Figure 4.** (A) Experimental and (B) simulated fit of the  $T_W$ -dependent 2DIR spectra of the CN-stretch of thiocyanate for aqueous solutions of 0.35 M NaNCS and 3 M CaI<sub>2</sub>. See text for description of the 2DIR spectra and Supporting Information for a description of the fitting procedure.

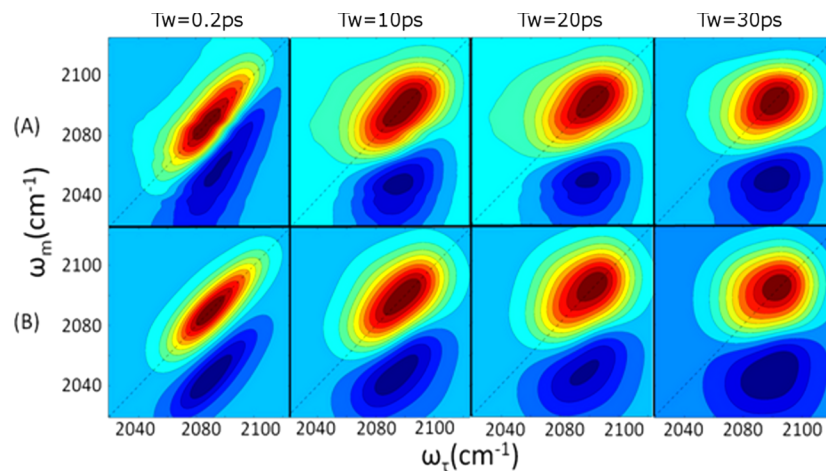


**Figure 5.** (A) Experimental and (B) simulated fit of the  $T_W$ -dependent 2DIR spectra of the CN-stretch of thiocyanate for aqueous solutions of 0.35 M NaNCS and 3 M CaI<sub>2</sub> and 3 M NaI. See text for description of the 2DIR spectra and Supporting Information for a description of the fitting procedure.

configuration during the  $T_W$  waiting time. This can be most obviously observed in the  $T_W = 40$  ps spectra in Figures 2A and 3A as shoulders to the main peaks at  $\omega_r = 2068 \text{ cm}^{-1}$ ,  $\omega_m = 2115 \text{ cm}^{-1}$  and  $\omega_r = 2115 \text{ cm}^{-1}$ ,  $\omega_m = 2032 \text{ cm}^{-1}$ . The additional cross peaks at  $\omega_r = 2115 \text{ cm}^{-1}$ ,  $\omega_m = 2068 \text{ cm}^{-1}$  and  $\omega_r = 2115 \text{ cm}^{-1}$ ,  $\omega_m = 2079 \text{ cm}^{-1}$  cannot be resolved in the spectra because they overlap with stronger diagonal and anharmonically shifted peaks. Figure 4A shows the absorptive 2DIR spectra for the 0.35 M NaNCS, 3 M CaI<sub>2</sub> solution, and Figure 5A shows the absorptive spectra for the 0.35 M NaNCS, 3 M CaI<sub>2</sub>, and 3 M NaI solution. The simulated fits to the experimental data appear in Figures 4B and 5B. The CN-stretch of the MgNCS<sup>+</sup> and CaNCS<sup>+</sup> CIP has a longer lifetime and orientational relaxation time than the CN-stretch of the free NCS<sup>-</sup> anion, leading to the change in intensity along the spectral diagonal. The chemical exchange between the free and CIP conformers appears primarily as a change in line shape from a diagonally elongated ellipsoid to a beveled square. We fully account for all eight distinct resonances in the 2DIR spectra with numerical modeling of the 2DIR spectra, as discussed in the Supporting Information.

### C. Kinetic Modeling of Ligand Exchange Dynamics.

The extraction of the ligand exchange reaction rates and

mechanism requires the full simulation of the  $T_W$ -dependent 2DIR spectra using the response function formalism based on diagrammatic perturbation theory<sup>46</sup> with input parameters estimated from the linear FTIR spectra and polarization resolved pump–probe measurements of the orientational and population relaxation rates. This methodology has been presented in detail previously,<sup>37,42,47</sup> and an overview of the methodology can be found in the Supporting Information. Here we present the kinetic modeling used to determine the ligand exchange mechanism.

Our measurement tracks the equilibrium conformational dynamics of the thiocyanate anions in solution, so we measure the equilibrium dynamics of the free NCS<sup>-</sup> and the MNCS<sup>+</sup> CIP. As demonstrated in a previous publication,<sup>38</sup> anion exchange dominates the chemical dynamics occurring on the tens of picoseconds time scale for  $[\text{NCS}^-] \leq 0.4 \text{ M}$ . Ignoring the activity coefficients of ionic species in solution, the equilibrium constant observed in spectroscopic measurements is given by

$$K_{\text{eq}} = \frac{[\text{MI}^+][\text{NCS}^-]}{[\text{MNCS}^+][\text{I}^-]} = \frac{k_{\text{diss}}}{k_{\text{asso}}} \quad (3)$$

where [...] represent the equilibrium concentrations. The  $[MNCS^+]$  and  $[NCS^-]$  can be determined from analysis of the FTIR and 2DIR spectra, as discussed in the Supporting Information.

The appropriate rate equation depends upon the reaction mechanism. For a *dissociative ligand exchange mechanism*, where the rate of  $MNCS^+$  dissociation does not depend upon the concentration of the  $I^-$  anion exchanging places with the  $NCS^-$  anion, the rate equations can be written as

$$\begin{aligned}\frac{d[MNCS^+]}{dt} &= -k_{\text{diss}}[MNCS^+] + k'_{\text{asso}}[M^{2+}][SCN^-] \\ \frac{d[SCN^-]}{dt} &= k_{\text{diss}}[MNCS^+] - k'_{\text{asso}}[M^{2+}][SCN^-]\end{aligned}\quad (4)$$

Since the  $[I^-]$  and  $[M^{2+}]$  concentrations exceed the  $NCS^-$  concentration by over an order of magnitude, we presume the  $[MI^+]$  concentration does not change significantly due to  $MNCS^+$  CIP formation. This allows the kinetics to be modeled as a pseudo-first-order reaction, with an effective association rate constant of  $k'_{\text{asso}} = k_{\text{asso}}[M^{2+}]$ . The rate equations for an *associative ligand exchange mechanism*, where the rate of  $MNCS^+$  dissociation depends linearly on the concentration of the  $I^-$  anion exchanging places with the  $NCS^-$  anion, can be written as

$$\begin{aligned}\frac{d[MNCS^+]}{dt} &= -k_{\text{diss}}[I^-][MNCS^+] + k'_{\text{asso}}[MI^+][SCN^-] \\ \frac{d[SCN^-]}{dt} &= k_{\text{diss}}[I^-][MNCS^+] - k'_{\text{asso}}[MI^+][SCN^-]\end{aligned}\quad (5)$$

Again, we presume the  $[MI^+]$  and the  $[I^-]$  concentrations do not change significantly due to  $MNCS^+$  CIP formation. Much like the dissociative reaction dynamics, this also allows the associative reaction to be modeled as a pseudo-first-order reaction with two effective rate constants,  $k'_{\text{asso}} = k_{\text{asso}}[MI^+]$  and  $k'_{\text{diss}} = k_{\text{diss}}[I^-]$ .

These rate equations can be analytically solved with the boundary condition,  $[SCN^-] + [MNCS^+] = \text{constant}$ , and the peak intensities in  $T_w$ -dependent 2DIR spectra are directly associated with the concentrations that are determined by the two-species exchange kinetics.<sup>15</sup>

$$\begin{aligned}[MNCS^+]_{\text{AA}}(T_w) &= [MNCS^+] \frac{k'_{\text{asso}} + k_{\text{diss}} \exp(-k_{\text{ex}} T_w)}{k_{\text{ex}}} \\ [SCN^-]_{\text{BB}}(T_w) &= [SCN^-] \frac{k_{\text{diss}} + k'_{\text{asso}} \exp(-k_{\text{ex}} T_w)}{k_{\text{ex}}} \\ [MNCS^+]_{\text{AB}}(T_w) &= [MNCS^+] \frac{k_{\text{diss}}(1 - \exp(-k_{\text{ex}} T_w))}{k_{\text{ex}}} \\ [SCN^-]_{\text{BA}}(T_w) &= [SCN^-] \frac{k'_{\text{asso}}(1 - \exp(-k_{\text{ex}} T_w))}{k_{\text{ex}}}\end{aligned}\quad (6)$$

where the exchange rate constant equals  $k_{\text{ex}} = k_{\text{diss}} + k'_{\text{asso}}$ ,  $[MNCS^+]_{\text{AA}}(T_w)$  and  $[SCN^-]_{\text{BB}}(T_w)$  are the concentrations associated with the diagonal peaks, and  $[MNCS^+]_{\text{AB}}(T_w)$  and  $[SCN^-]_{\text{BA}}(T_w)$  are the concentrations associated with the cross peaks. Note for modeling the associative reaction, we replace  $k_{\text{diss}}$  with  $k'_{\text{diss}} = k_{\text{diss}}[I^-]$ .

The kinetic equations show that the secondary anion concentration dependence of the  $[MNCS^+]$  dissociation provides a clear means of determining whether the ligand exchange process follows a dissociative or an associative reaction mechanism. The limited dynamic range of the 2DIR measurements due to the CN-stretch vibrational lifetime constrains the secondary ion concentration range we can access experimentally. For  $Mg^{2+}$  we have varied the  $[I^-]$  concentration by nearly a factor of 2 from 6 to 10.4 M, while keeping the  $[NCS^-]$  and the  $[Mg^{2+}]$  concentrations constant. As can be seen in Figures 2A and 3A, changing the iodide concentration has minimal effect on the exchange dynamics. Figures 2B and 3B show the detailed fits of the experimental data. The fits to the 2DIR spectra give a forward reaction time constant for  $MgNCS^+$  dissociation that does not vary significantly with  $[I^-]$  ( $82 \pm 8$  ps for 6 M  $I^-$  and  $75 \pm 7$  ps for 10.4 M  $I^-$ ). All the rates extracted from the data analysis can be found in Table 1. The  $T_w$ -dependent peak volumes extracted from the 2DIR spectra and a description of the error analysis can be found in the Supporting Information.

**Table 1. Exchange Rates for Aqueous Solutions of 3 M  $Mg^{2+}$**

	$I^-$	NCS <sup>-</sup>		
		0.12 M	0.24 M	0.4 M
6 M				
	$[k_{\text{diss}}]^{-1}$ (ps)	$85 \pm 8$	$82 \pm 8$	$87 \pm 9$
	$[k'_{\text{asso}}]^{-1}$ (ps)	$212 \pm 20$	$233 \pm 20$	$247 \pm 24$
10.4 M				
	$[k_{\text{diss}}]^{-1}$ (ps)		$75 \pm 7$	
	$[k'_{\text{asso}}]^{-1}$ (ps)		$120 \pm 12$	

The experimental measurements and fits for aqueous solutions containing  $Ca^{2+}$  and  $NCS^-$  appear in Figures 4 and 5. For  $Ca^{2+}$  we have varied the  $[I^-]$  concentration by a factor of 1.5, while keeping the  $[NCS^-]$  and the  $[Ca^{2+}]$  concentrations constant, and observed the time constant for  $CaNCS^+$  dissociation decrease by a factor of 1.4 ( $75 \pm 12$  ps for 6 M  $I^-$  and  $55 \pm 10$  ps for 9 M  $I^-$ ). The forward and back reaction time constants for all solutions can be found in Table 2. The

**Table 2. Exchange Rates for Aqueous Solutions of 3 M  $Ca^{2+}$**

	$I^-$	NCS <sup>-</sup>	
		0.35 M	
7 M		$[k_{\text{diss}}]^{-1}$ (ps)	$75 \pm 12$
10.5 M		$[k'_{\text{asso}}]^{-1}$ (ps)	$130 \pm 20$
			$55 \pm 10$
			$80 \pm 13$

expected increase in rate for an associative reaction cannot be determined solely from the change in total  $[I^-]$  concentration. The rate should be proportional to the concentration of free  $I^-$ , not total  $I^-$  in solution. Increasing the concentration of  $I^-$  will shift the equilibrium toward  $CaI^+$ . This means the ratio of the rates should be less than 1.5, but how much less cannot be determined without knowing the equilibrium constant for  $CaI^+$  association. Despite this uncertainty, the clear increase in rate with increased iodide concentration demonstrates that associative ligand exchanges dominate the kinetics for  $Ca^{2+}$  in aqueous solution.

Table 1 and Table 2 demonstrate that the rate of  $M^{2+}$  and  $NCS^-$  association depends on the  $I^-$  concentration for both  $Mg^{2+}$  and  $Ca^{2+}$ . These observations cannot be utilized as readily to extract mechanistic information because the association rate

depends directly on the unknown concentration of  $\text{MI}^+$  in solution. For  $\text{MgNCS}^+$  dissociation, this detail has no impact on the observed reaction rate because the rate does not depend on the  $[\text{I}^-]$  concentration. For  $\text{Mg}^{2+}$  and  $\text{NCS}^-$  association, the rate does depend on the  $[\text{I}^-]$  concentration. We presume this dependence derives from the fact that the probability of finding undercoordinated  $\text{Mg}^{2+}$  cations increases with the increase in  $\text{I}^-$  filled coordination sites. This can be seen in the  $[\text{I}^-]$  concentration dependence for the association rates listed in Table 1. As mentioned above, the associative mechanism for  $\text{CaNCS}^+$  dissociation makes the dissociation rate depend indirectly on the  $\text{MI}^+$  concentration because we control the total  $[\text{I}^-]$  concentration in solution, but cannot control the fraction of  $\text{I}^-$  that resides in  $\text{CaI}^+$  CIP. For  $\text{Ca}^{2+}$  and  $\text{NCS}^-$  association, the rate depends directly on the  $[\text{CaI}^+]$  concentration, which increases with increasing  $[\text{I}^-]$ .

#### IV. DISCUSSION

The exchange mechanism into and out of the first solvation shell of  $\text{Mg}^{2+}$  has been investigated experimentally with NMR, ultrasonic absorption spectroscopy, and molecular dynamics simulations.<sup>4,8,12,48,49</sup> All these methods, with the exception of NMR, have also been used to study water exchange into and out of the first solvation shell of  $\text{Ca}^{2+}$ . Molecular dynamics simulations observe that the free energy of hypercoordinated  $\text{Mg}^{2+}\cdot 7\text{H}_2\text{O}$  significantly exceeds the free energy of the hypocoordinated  $\text{Mg}^{2+}\cdot \text{SH}_2\text{O}$ .<sup>12</sup> Using the same simulation methodology, the reverse holds true for  $\text{Ca}^{2+}$ , where hypercoordinated configurations have lower free energies than hypocoordinated configurations. The simulation results agree with the interpretation of  $\text{MgSO}_4$  ion pairing dynamics measured with ultrasonic absorption<sup>4</sup> and the interpretation of activation volumes measured with pressure dependent NMR.<sup>2,49</sup> Unlike  $\text{Mg}^{2+}$ , no clear consensus exists for the exchange mechanism for  $\text{Ca}^{2+}$ . The variation in exchange mechanism agrees with that extracted from the MD simulations of Ikeda, Boero, and Terakura.<sup>12</sup> These results strongly indicate that the flexibility of the first solvation shell dictates the exchange mechanism.  $\text{Mg}^{2+}$  has a well-defined octahedral coordination in aqueous solution, while  $\text{Ca}^{2+}$  has a much broader coordination number distribution with appreciable concentrations of  $\text{Ca}^{2+}$  cations with six, seven, and even eight ligands at equilibrium. The self-consistent explanation for our measurements and the molecular dynamics simulations of isolated  $\text{Mg}^{2+}$  and  $\text{Ca}^{2+}$  cations indicate that the mechanisms observed for concentrated solutions also apply in more dilute solutions.

The lack of a significant chemical shift for water when binding to  $\text{Ca}^{2+}$  makes NMR insensitive to water exchange, and the water exchange rates extracted from MD simulations,<sup>2</sup> quasi-elastic neutron scattering (QENS),<sup>50</sup> and ultrasonic absorption spectroscopy<sup>4</sup> measurements differ significantly. Various experiments have been interpreted to be consistent with water residence times ranging from less than 150 ps<sup>50</sup> to roughly 100 ns,<sup>4</sup> and MD simulations have extracted residence times ranging from 15 to 150 ps.<sup>9</sup> Our measurements put a lower bound on the water- $\text{NCS}^-$  exchange of roughly 75 ps. In conjunction with the QENS results of Salmon et al.,<sup>50</sup> we attribute a residence time for water of roughly 100 ps in the first solvation shell of  $\text{Ca}^{2+}$ . This rate of water exchange exceeds the rate extracted from ultrasonic absorption spectroscopy<sup>4</sup> by 3 orders of magnitude, but agrees with MD simulation results.<sup>9</sup> Our observations confirm that the exchange of a water

molecule into and out of the first solvation shell occurs roughly 5 orders of magnitude faster for  $\text{Ca}^{2+}$  than  $\text{Mg}^{2+}$ . Despite the enormous difference in the residence times for water, the anion residence times vary surprisingly little between  $\text{Ca}^{2+}$  and  $\text{Mg}^{2+}$ . These findings indicate that some combination of polarizability or electron transfer must be included in the MD simulation to accurately treat ion solvation and contact ion formation and bring into question the applicability of nonpolarizable MD force fields for describing ion channels and many other biological phenomena that require an accurate description of ion solvation and contact ion pair formation.<sup>1,51–53</sup>

#### V. CLOSING REMARKS

We have utilized 2DIR spectroscopy to investigate the ligand exchange mechanism and dynamics for aqueous  $\text{Mg}^{2+}$  and  $\text{Ca}^{2+}$  cations. We have determined that anion exchange follows a dissociative mechanism for  $\text{Mg}^{2+}$  and an associative mechanism for  $\text{Ca}^{2+}$ , at least in concentrated aqueous ionic solutions. Surprisingly, the rates of contact ion pair dissociation between monovalent anions and  $\text{Mg}^{2+}$  and  $\text{Ca}^{2+}$  cations differ by less than a factor of 2, but the rate of dissociation for  $\text{Ca}^{2+}$  and water exceeds the rate for  $\text{Mg}^{2+}$  and water by roughly 5 orders of magnitude. While the significant difference in the stability of  $\text{Mg}^{2+}$ -water and  $\text{Ca}^{2+}$ -water complexes has long been presumed from prior measurements, the interaction of  $\text{Mg}^{2+}$  and  $\text{Ca}^{2+}$  with counterions has not been as widely investigated. How these ligand exchange rates and mechanisms influence cation recognition can only be speculated about at present, but recent crystallography studies of the  $\text{Ca}^{2+}$  ion pump  $\text{Ca}^{2+}$ -ATPase present intriguing possibilities.<sup>54,55</sup> Rather than inhibiting  $\text{Ca}^{2+}$  binding,  $\text{Mg}^{2+}$  can accelerate  $\text{Ca}^{2+}$  in this ion pump protein. The crystal structures indicate that  $\text{Mg}^{2+}$  ions bind in one of the two  $\text{Ca}^{2+}$  binding sites, yet freely exchange with  $\text{Ca}^{2+}$  ions when they are both present in the cytosol. Presumably the free energy for the  $\text{Mg}^{2+}$  and  $\text{Ca}^{2+}$  interactions with the charged and dipolar protein functional groups must be similar, as we see for  $\text{Mg}^{2+}$  and  $\text{Ca}^{2+}$  interactions with monovalent anions, and quite dissimilar from their interactions with water.

#### ■ ASSOCIATED CONTENT

##### Supporting Information

The polarization resolved vibrational pump-probe measurements of vibrational lifetimes and orientational relaxation and a detailed discussion of the numerical modeling of the experimental results. This material is available free of charge via the Internet at <http://pubs.acs.org>.

#### ■ AUTHOR INFORMATION

##### Corresponding Author

\*K.J.G.: SLAC National Accelerator Laboratory, Menlo Park, CA 94025; phone, 650-926-2382; e-mail, kgaffney@SLAC.Stanford.edu.

##### Present Address

<sup>†</sup>M.J.: Department of Chemistry and Chemical Biology, Harvard University, Cambridge, Massachusetts 02138, United States.

##### Notes

The authors declare no competing financial interest.

## ACKNOWLEDGMENTS

This research is supported through the AMOS program within the Chemical Sciences, Geosciences, and Biosciences Division of the Office of Basic Energy Sciences, Office of Science, U.S. Department of Energy.

## REFERENCES

- (1) Aqvist, J.; Luzhkov, V. B.; Brandsdal, B. O. Ligand Binding Affinities from MD Simulations. *Acc. Chem. Res.* **2002**, *35*, 358–365.
- (2) Helm, L.; Merbach, A. E. Water Exchange on Metal Ions: Experiments and Simulations. *Coord. Chem. Rev.* **1999**, *187*, 151–181.
- (3) Helm, L.; Merbach, A. E. Inorganic and Bioinorganic Solvent Exchange Mechanisms. *Chem. Rev.* **2005**, *105*, 1923–1959.
- (4) Eigen, M. Fast Elementary Steps in Chemical Reaction Mechanisms. *Pure Appl. Chem.* **1963**, *6*, 97–116.
- (5) Buchner, R. What Can Be Learnt from Dielectric Relaxation Spectroscopy About Ion Solvation and Association? *Pure Appl. Chem.* **2008**, *80*, 1239–1252.
- (6) Buchner, R.; Chen, T.; Hefter, G. Complexity in "Simple" Electrolyte Solutions: Ion Pairing in  $MgSO_4(Aq)$ . *J. Phys. Chem. B* **2004**, *108*, 2365–2375.
- (7) Laage, D.; Hynes, J. T. On the Residence Time for Water in a Solute Hydration Shell: Application to Aqueous Halide Solutions. *J. Phys. Chem. B* **2008**, *112*, 7697–7701.
- (8) Rode, B. M.; Schwenk, C. F.; Hofer, T. S.; Randolph, B. R. Coordination and Ligand Exchange Dynamics of Solvated Metal Ions. *Coord. Chem. Rev.* **2005**, *249*, 2993–3006.
- (9) Lim, L. H. V.; Prebil, A. B.; Ellmerer, A. E.; Randolph, B. R.; Rode, B. M. Temperature Dependence of Structure and Dynamics of the Hydrated  $Ca^{2+}$  Ion According to Ab Initio Quantum Mechanical Charge Field and Classical Molecular Dynamics. *J. Comput. Chem.* **2009**, *31*, 1195–1200.
- (10) Fennell, C. J.; Bizjak, A.; Vlachy, V.; Dill, K. A. Ion Pairing in Molecular Simulations of Aqueous Alkali Halide Solutions. *J. Phys. Chem. B* **2009**, *113*, 6782–6791.
- (11) Smith, D. E.; Dang, L. X. Computer-Simulations of NaCl Association in Polarizable Water. *J. Chem. Phys.* **1994**, *100*, 3757–3766.
- (12) Ikeda, T.; Boero, M.; Terakura, K. Hydration Properties of Magnesium and Calcium Ions from Constrained First Principles Molecular Dynamics. *J. Chem. Phys.* **2007**, *127*, 074503.
- (13) Bakker, H. J. Structural Dynamics of Aqueous Salt Solutions. *Chem. Rev.* **2008**, *108*, 1456–1473.
- (14) Tielrooij, K. J.; Garcia-Araez, N.; Bonn, M.; Bakker, H. J. Cooperativity in Ion Hydration. *Science* **2010**, *328*, 1006–1009.
- (15) Park, S.; Ji, M. B.; Gaffney, K. J. Ligand Exchange Dynamics in Aqueous Solution Studied with 2DIR Spectroscopy. *J. Phys. Chem. B* **2010**, *114*, 6693–6702.
- (16) Ji, M. B.; Odelius, M.; Gaffney, K. J. Large Angular Jump Mechanism Observed for Hydrogen Bond Exchange in Aqueous Perchlorate Solution. *Science* **2010**, *328*, 1003–1005.
- (17) Ji, M. B.; Gaffney, K. J. Orientational Relaxation Dynamics in Aqueous Ionic Solution: Polarization-Selective Two-Dimensional Infrared Study of Angular Jump-Exchange Dynamics in Aqueous 6M  $NaClO_4$ . *J. Chem. Phys.* **2011**, *134*, 044516.
- (18) Park, S.; Odelius, M.; Gaffney, K. J. Ultrafast Dynamics of Hydrogen Bond Exchange in Aqueous Ionic Solutions. *J. Phys. Chem. B* **2009**, *113*, 7825–7835.
- (19) Ji, M. B.; Hartsock, R. W.; Sun, Z.; Gaffney, K. J. Interdependence of Conformational and Chemical Reaction Dynamics During Ion Assembly in Polar Solvents. *J. Phys. Chem. B* **2011**, *115*, 11399–11408.
- (20) Gaffney, K. J.; Ji, M. B.; Odelius, M.; Park, S.; Sun, Z. H-Bond Switching and Ligand Exchange Dynamics in Aqueous Ionic Solution. *Chem. Phys. Lett.* **2011**, *504*, 1–6.
- (21) Moilanen, D. E.; Wong, D.; Rosenfeld, D. E.; Fenn, E. E.; Fayer, M. D. Ion-Water Hydrogen-Bond Switching Observed with 2D IR Vibrational Echo Chemical Exchange Spectroscopy. *Proc. Natl. Acad. Sci. U.S.A.* **2009**, *106*, 375–380.
- (22) Park, S.; Moilanen, D. E.; Fayer, M. D. Water Dynamics - the Effects of Ions and Nanoconfinement. *J. Phys. Chem. B* **2008**, *112*, 5279–5290.
- (23) Bian, H. T.; Wen, X. W.; Li, J. B.; Chen, H. L.; Han, S. Z.; Sun, X. Q.; Song, J. A.; Zhuang, W.; Zheng, J. R. Ion Clustering in Aqueous Solutions Probed with Vibrational Energy Transfer. *Proc. Natl. Acad. Sci. U.S.A.* **2011**, *108*, 4737–4742.
- (24) Kuroda, D. G.; Hochstrasser, R. M. Dynamic Structures of Aqueous Oxalate and the Effects of Counterions Seen by 2D IR. *Phys. Chem. Chem. Phys.* **2012**, *14*, 6219–6224.
- (25) Callahan, K. M.; Casillas-Ituarte, N. N.; Roeselova, M.; Allen, H. C.; Tobias, D. J. Solvation of Magnesium Dication: Molecular Dynamics Simulation and Vibrational Spectroscopic Study of Magnesium Chloride in Aqueous Solutions. *J. Phys. Chem. A* **2010**, *114*, 5141–5148.
- (26) Getahun, Z.; Huang, C. Y.; Wang, T.; De Leon, B.; DeGrado, W. F.; Gai, F. Using Nitrile-Derivatized Amino Acids as Infrared Probes of Local Environment. *J. Am. Chem. Soc.* **2003**, *125*, 405–411.
- (27) Waegele, M. M.; Culik, R. M.; Gai, F. Site-Specific Spectroscopic Reporters of the Local Electric Field, Hydration, Structure, and Dynamics of Biomolecules. *J. Phys. Chem. Lett.* **2011**, *2*, 2598–2609.
- (28) Levinson, N. M.; Fried, S. D.; Boxer, S. G. Solvent-Induced Infrared Frequency Shifts in Aromatic Nitriles Are Quantitatively Described by the Vibrational Stark Effect. *J. Phys. Chem. B* **2012**, *116*, 10470–10476.
- (29) Boxer, S. G. Stark Realities. *J. Phys. Chem. B* **2009**, *113*, 2972–2983.
- (30) Reimers, J. R.; Hall, L. E. The Solvation of Acetonitrile. *J. Am. Chem. Soc.* **1999**, *121*, 3730–3744.
- (31) Choi, J. H.; Oh, K. I.; Lee, H.; Lee, C.; Cho, M. Nitrile and Thiocyanate IR Probes: Quantum Chemistry Calculation Studies and Multivariate Least-Square Fitting Analysis. *J. Chem. Phys.* **2008**, *128*, 134506.
- (32) Ji, M. B.; Park, S.; Gaffney, K. J. Dynamics of Ion Assembly in Solution: 2DIR Spectroscopy Study of LiNCS in Benzonitrile. *J. Phys. Chem. Lett.* **2010**, *1*, 1771–1775.
- (33) Son, H.; Jin, H.; Choi, S. R.; Jung, H. W.; Park, S. Infrared Probing of Equilibrium and Dynamics of Metal-Selenocyanate Ion Pairs in N,N-Dimethylformamide Solutions. *J. Phys. Chem. B* **2012**, *116*, 9152–9159.
- (34) Asplund, M. C.; Zanni, M. T.; Hochstrasser, R. M. Two-Dimensional Infrared Spectroscopy of Peptides by Phase-Controlled Femtosecond Vibrational Photon Echoes. *Proc. Natl. Acad. Sci. U.S.A.* **2000**, *97*, 8219–8224.
- (35) Graener, H.; Dohlus, R.; Laubereau, A. Infrared Double-Resonance Spectroscopy of Bromoform with Picosecond Pulses. *Chem. Phys. Lett.* **1987**, *140*, 306–310.
- (36) Hamm, P.; Lim, M.; DeGrado, W. F.; Hochstrasser, R. M. The Two-Dimensional IR Nonlinear Spectroscopy of a Cyclic Pentapeptide in Relation to Its Three-Dimensional Structure. *Proc. Natl. Acad. Sci. U.S.A.* **1999**, *96*, 2036–2041.
- (37) Khalil, M.; Demirdoven, N.; Tokmakoff, A. Coherent 2D IR Spectroscopy: Molecular Structure and Dynamics in Solution. *J. Phys. Chem. A* **2003**, *107*, 5258–5279.
- (38) Sun, Z.; Zhang, W. K.; Ji, M. B.; Hartsock, R. W.; Gaffney, K. J. Contact Ion Pair Formation between Hard Acids and Soft Bases in Aqueous Solutions Observed with 2DIR Spectroscopy. *J. Phys. Chem. B* **2013**, DOI: jp4033854.
- (39) Woutersen, S.; Bakker, H. J. Resonant Intermolecular Transfer of Vibrational Energy in Liquid Water. *Nature* **1999**, *402*, 507–509.
- (40) Gaffney, K. J.; Piletic, I. R.; Fayer, M. A. Orientational Relaxation and Vibrational Excitation Transfer in Methanol – Carbon Tetrachloride Solutions. *J. Chem. Phys.* **2003**, *118*, 2270–2278.
- (41) Phutela, R. C.; Pitzer, K. S. Thermodynamics of Aqueous Calcium-Chloride. *J. Solution Chem.* **1983**, *12*, 201–207.

- (42) Park, S.; Kwak, K.; Fayer, M. D. Ultrafast 2D-IR Vibrational Echo Spectroscopy: A Probe of Molecular Dynamics. *Laser Phys. Lett.* **2007**, *4*, 704–718.
- (43) Schultz, P. W.; Leroi, G. E.; Harrison, J. F. Ab Initio Calculations of Ionic and Hydrogen Bonding Interactions with the OCN<sup>-</sup>, SCN<sup>-</sup> and SeCN<sup>-</sup> Anions. *Mol. Phys.* **1996**, *88*, 217–246.
- (44) Squalli, O.; Costa, M. C. M.; Cartier, A.; Chabanel, M. A Molecular-Orbital Study of Bonding and Frequency-Shifts in Free and Solvated Lithium Thiocyanate Aggregates. *J. Mol. Struct. THEOCHEM* **1994**, *109*, 11–18.
- (45) Buchner, R.; Capewell, S. G.; Hefter, G.; May, P. M. Ion-Pair and Solvent Relaxation Processes in Aqueous Na<sub>2</sub>SO<sub>4</sub> Solutions. *J. Phys. Chem. B* **1999**, *103*, 1185–1192.
- (46) Mukamel, S. *Principles of Nonlinear Optical Spectroscopy*; Oxford University Press: New York, 1995.
- (47) Kwak, K.; Zheng, J. R.; Cang, H.; Fayer, M. D. Ultrafast Two-Dimensional Infrared Vibrational Echo Chemical Exchange Experiments and Theory. *J. Phys. Chem. B* **2006**, *110*, 19998–20013.
- (48) Tongraar, A.; Rode, B. M. Structural Arrangement and Dynamics of the Hydrated Mg<sup>2+</sup>: An Ab Initio QM/MM Molecular Dynamics Simulation. *Chem. Phys. Lett.* **2005**, *409*, 304–309.
- (49) Bleuzen, A.; Pittet, P. A.; Helm, H.; Merbach, A. E. Water Exchange on Magnesium(II) in Aqueous Solution: A Variable Temperature and Pressure O-17 NMR Study. *Magn. Reson. Chem.* **1997**, *35*, 765–773.
- (50) Salmon, P. S. The Dynamics of Water-Molecules in Ionic Solution as Studied by Incoherent Quasi-Elastic Neutron-Scattering. *Physica B* **1989**, *156*, 129–131.
- (51) Warshel, A.; Kato, M.; Pisliakov, A. V. Polarizable Force Fields: History, Test Cases, and Prospects. *J. Chem. Theory Comput.* **2007**, *3*, 2034–2045.
- (52) Warshel, A.; Sharma, P. K.; Kato, M.; Parson, W. W. Modeling Electrostatic Effects in Proteins. *Biochim. Biophys. Acta* **2006**, *1764*, 1647–1676.
- (53) Thompson, W. H.; Hynes, J. T. Frequency Shifts in the Hydrogen-Bonded Oh Stretch in Halide-Water Clusters. The Importance of Charge Transfer. *J. Am. Chem. Soc.* **2000**, *122*, 6278–6286.
- (54) Toyoshima, C. Structural Aspects of Ion Pumping by Ca<sup>2+</sup>-ATPase of Sarcoplasmic Reticulum. *Arch. Biochem. Biophys.* **2008**, *476*, 3–11.
- (55) Toyoshima, C.; Iwasawa, S.; Ogawa, H.; Hirata, A.; Tsueda, J.; Inesi, G. Crystal Structures of the Calcium Pump and Sarcolipin in the Mg<sup>2+</sup>-Bound E1 State. *Nature* **2013**, *495*, 260–264.